Journal of Thermal Analysis and Calorimetry, Vol. 80 (2005) 549–553

FLAME PROPAGATION OVER LIQUID ALCOHOLS
Part II. Steady propagation regimes

E. Degroote[1*] *and P. L. García Ybarra*[2]

[1]Universidad Politécnica de Madrid, Dep. Ciencia y Tecnología Aplicadas, E. U. I. T. Agrícolas, Ciudad Universitaria, s/n. 28040 Madrid, Spain
[2]CIEMAT, Av. Complutense, 22, 28040 Madrid, Spain

The different spreading regimes above liquid fuels have been experimentally characterized for surface temperatures close to the flash-point temperature. Two different spreading regimes are observed: for temperatures larger than some critical value, flame spreading velocity is well described by the De Ris solid fuel-like model. For temperature values lower than the critical one, a preheating thermocapillary region has been observed in the fuel, which can be described by a purely thermodynamic non-reactive model. The critical transition temperature has shown to present common characteristics for the four alcohols used in the experiments.

Keywords: *combustion, flame spreading, fuels, heat transfer, temperature*

Introduction

Flame spreading over liquid fuels is usually accompanied by liquid fuel motions generated by the thermocapillary effect [1]. The heating of the liquid fuel under the flame tip produces surface tension gradients that can lead to motions in the liquid bulk by viscous stresses. This is a distinctive characteristic with respect to flame spreading above a solid fuel and provides a mechanism to promote the flame spreading. Akita [2] pointed out the different regimes exhibited by a flame spreading above alcohols in channels, as depicted in Fig. 1. This particular case corresponds to a flame spreading over ethanol in a channel of 2.5 cm width; in this plot, squares represent maximum spreading velocities and diamonds are the minimum velocities. As shown by the figure, for large values of the initial surface fuel temperature, $T_0>T_1$, the fuel vapor pressure is very high, and leads to a flame spreading regime purely controlled by the gas phase, ignoring the presence of the liquid fuel. Flame propagation velocities of the order of 100 cm s^{-1} are observed in this region. For relatively high temperatures $T_2<T_0<T_1$, a regime of uniform flame spreading velocity, controlled by heat diffusion in the condensed phase appears (similar to the solid case). Flame velocity v_f decreases almost linearly with decreasing temperatures (this dependence can be extended to the logarithm of v_f with a lower correlation) and the slope is in this region of order of 10 cm s^{-1} $^oC^{-1}$. For even lower temperatures, that is for $T_3<T_0<T_2$, a new uniform regime is observed, but in this case the slope of the T_0–v_f diagram is of order 1.0 cm s^{-1} $°C^{-1}$; an abrupt transition with respect to the preceding regime is observed. The fuel temperature T_2 defines the transition value that should be considered as a transcritical bifurcation point of the whole system; it corresponds to the critical value where flame propagation (previously controlled by heat diffusion in the condensed phase) turns to flame propagation assisted by heat convection in the liquid fuel. Thermocapillary convection brings hot fuel ahead of the flame tip and a vortex of warm liquid fuel develops there [3, 4] which, as we will see below, enhances flame spreading by reducing flame heat losses. For $T_4<T_0<T_3$, the flame spreading exhibits oscillatory behavior. A limit cycle appears at $T_0=T_3$, as a Hopf bifurcation from the thermocapillary assisted spreading regime known as the pulsating regime [2]. Finally, for temperatures $T_0<T_4$, flame spreading velocity is almost constant, with values close to 1 cm s^{-1}. The critical point T_4 corresponds to a homoclinic orbit, where a divergence in the period is observed. The features of this steady state flame spread driven by the thermocapillary effect have been described in [5] and computer codes have been developed for this propagation mode [6, 7]. This sequence of transitions between different spreading regimes has been the subject of a large number of works [2, 6–12], but the fundamental mechanisms involved are not well known, specially in the uniform regimes. The purpose of this work is to contribute to the understanding of the steady regimes of flame spreading when both phases, liquid and gas, are initially at rest and the surface temperature is kept uniformly constant at some initial value T_0 that will be varied around T_2, corresponding then to $T_3<T_0<T_1$.

* Author for correspondence: eugenio.degroote@upm.es

1388–6150/$20.00

Akadémiai Kiadó, Budapest, Hungary
Springer, Dordrecht, The Netherlands

Experimental

The experimental setup consists of an open channel configuration, filled with a liquid fuel. The initial fuel temperature was kept uniform along the horizontal with a refrigerant circuit. Four aliphatic alcohols (methanol, ethanol, 2-propanol and 1-butanol) and two different channel lengths have been used (40×4.0×2.5 cm and 100×1.5×3.4 cm, respectively). Two different kinds of lateral walls were employed (aluminium and Pyrex). Eight thermocouples (Cr–Al, ϕ=25 μm), regularly spaced along the fuel surface, record the evolution of the fuel surface temperature; a video camera provides the flame front evolution and its spreading velocity (more details can be found in [14]).

The spreading velocity of the flame can then be represented as a function of T_0 as a bifurcation diagram. A typical plot of the flame spreading velocities for ethanol in the 40 cm long channel (with lateral walls made of aluminium) is shown in Fig. 1. Qualitatively identical results have been observed for all of the alcohols and channels.

Steady propagation regimes

Results

Table 1 shows the different values obtained for T_1, T_2 and T_3 for the four alcohols in a 40 cm long channel, with lateral walls made of Pyrex; a plot of the flame velocity in these regimes for butanol is shown in Fig. 2. The value T_2=36.1ºC, corresponding to the abrupt change in slope, is close to the well-known flashpoint temperature (T_{flash}). This coincidence has been noted and discussed in previous works [2]. However, it has to be observed that T_2 and T_{flash} characterize two completely different phenomena; the first case corresponds to a dynamic energy balance leading to the spreading of the flame, while the second case corresponds to the initiation of a flame under some standard conditions.

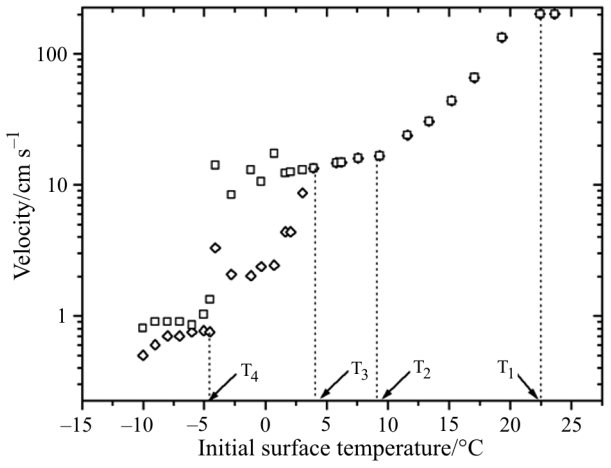

Fig. 1 Bifurcation diagram for the flame spreading velocity over ethanol

Table 1 Critical temperatures T_1, T_2, T_3 with lateral walls made of aluminium. The last line corresponds to the flash-point temperature

T/°C	Methanol	Ethanol	Propanol	Butanol
T_1	20.5	22.5	32.7	37.9
T_2	9.3	9.5	17.5	36.1
T_3	–1.9	3.5	5.9	24.1
T_{flash}	11.0	13.0	25.0	29.0

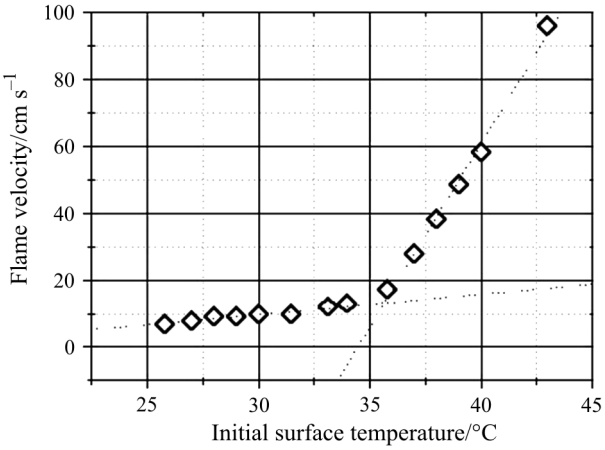

Fig. 2 Flame velocity plot in the steady region for butanol. Diamonds represent experimental results, and dotted lines correspond to the fit in every region

During the flame spreading experiments in these regimes, the temperature records of each thermocouple experience an abrupt increase with the passage of the flame. Furthermore, in the thermocapillary assisted regime ($T_3<T_0<T_2$) a slight temperature augmentation preceding flame arrival was detected before this abrupt increase in the temperature, indicating the existence of a preheated region of warm liquid fuel ahead of the flame tip, as pointed out in the introduction. In spite of the limited accuracy of the temperature measurement technique (surface thermocouples), an approximate measure of the horizontal length L of this preheat region *vs*. the initial fuel temperature is shown in Fig. 3. No characteristic length L vanishes for values close to T_2, whereas near T_3 it is close to 1 cm. On the other hand, for fuel temperature values $T_0>T_2$, corresponding to the solid fuel-like regime, no detectable increase in the liquid temperature has been observed before flame arrival. These findings agree with the results reported by Ito *et al*. [3] and Ross *et al*. [4] (they observed a well developed vortex preceding the flame only in the thermocapillary assisted spreading regime).

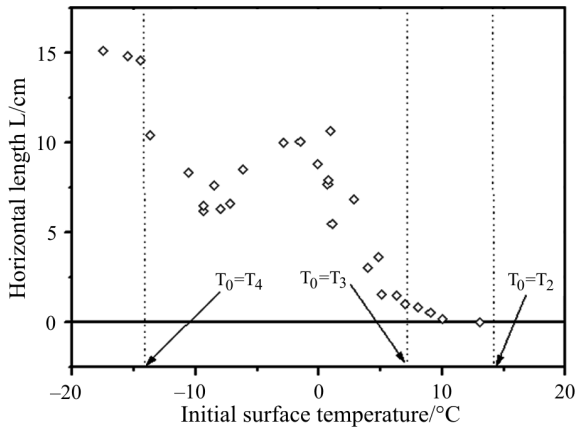

Fig. 3 Characteristic length L of the preheated vortex *vs*. initial fuel surface temperature T_0

Solid fuel-like propagation regime: $T_0 > T_2$

In this region, flame spreading velocity is very large compared to any thermocapillary or gravity induced liquid motion, and the spreading proceeds similarly to flame spread on a solid fuel. Let q_g be the order of magnitude of the heat flux in the gas phase near the flame tip:

$$q_g \approx \lambda_g \frac{\Delta T_g}{\delta_{nsg}} \tag{1}$$

and q_l the corresponding order of magnitude of the heat flux in the liquid fuel underneath the gas,

$$q_l \approx \lambda_l \frac{\Delta T_l}{\delta_T} \tag{2}$$

where λ_g is the gas thermal conductivity, λ_l the liquid thermal conductivity, δ_{nsg} is the characteristic size of the Navier–Stokes region (in the gas phase) and ΔT_g is the thermal layer thickness (in the liquid phase) [12]. The typical temperature differences, ΔT_g (in the gas phase) and ΔT_l (in the liquid phase) are

$$\begin{aligned} \Delta T_g &\approx T_f - T_0 \\ \Delta T_l &\approx T_b - T_0 \end{aligned} \tag{3}$$

where T_b is the fuel boiling temperature, and T_f the corresponding flame temperature. Then, the balance between q_g and q_l leads to the relation

$$\delta_T \approx \frac{\lambda_l}{\lambda_g} \frac{\Delta T_l}{\Delta T_g} \delta_{nsg} \tag{4}$$

Additionally, the order of δ_{nsg} is given by

$$\delta_{nsg} \approx \frac{v_g}{u_{nsg}} \tag{5}$$

where u_{nsg} is the order of the local velocity in the Navier–Stokes region around the flame tip in the gas phase. On the other hand, by assuming a thin layer structure in the liquid, the convective–diffusive heat balance obtained from the equation

$$\rho_l c_{pl} v_f \frac{\partial T}{\partial x} = \lambda_l \frac{\partial^2 T}{\partial y^2} \tag{6}$$

gives

$$\rho_l c_{pl} v_f \frac{\Delta T_l}{\delta_{nsg}} \approx \lambda_l \frac{\Delta T}{\delta_T^2} \tag{7}$$

and leads to

$$\delta_T \approx \sqrt{\frac{\lambda_l}{\rho_l c_{pl} v_f} \delta_{nsg}} \tag{8}$$

By comparing with Eq. (4), and considering that the Prandtl number in the gas phase is close to unity, the following relation for the flame spreading velocity v_f is obtained:

$$v_f \approx u_{nsg} \frac{\lambda_g \rho_g c_{pg}}{\lambda_l \rho_l c_{pl}} \left(\frac{\Delta T_g}{\Delta T_l} \right)^2 \tag{9}$$

This result agrees with the De Ris relation for flame spreading over solid fuel [13]. Assuming that buoyancy is the driving mechanism for the gas flow around the flame, the momentum balance in the gas phase is

$$\frac{u_{nsg}^2}{\lambda_g / (\rho_g c_{pg} u_{nsg})} \approx \frac{\Delta \rho_g}{\rho_g} g \tag{10}$$

This relation provides the magnitude of the velocity u_{nsg}

$$u_{nsg} \approx \left(g \frac{T_f - T_0}{T_0} \frac{\lambda_g}{\rho_g c_{pg}} \right)^{1/3} \tag{11}$$

Moreover, assuming that we have (according to kinetic theory of gases)

$$\lambda_g \approx \sqrt{T_0}; \rho_g \approx \frac{1}{T_0} \tag{12}$$

The following relation between T_0 and v_f

$$v_f \approx \frac{T_0^{1/6}}{T_0^{1/2}} \frac{1}{(\Delta T_l)^2} = \frac{1}{T_0^{1/3} (T_b - T_0)^2} \tag{13}$$

In order to check the suitability of this last relation for this region, a linear fit between the variables

$$x = \frac{1}{T_0^{1/3} (T_b - T_0)^2}; \; y = v_f \tag{14}$$

has been performed for our experimental results in the 40 cm long channel with side walls made of Pyrex.

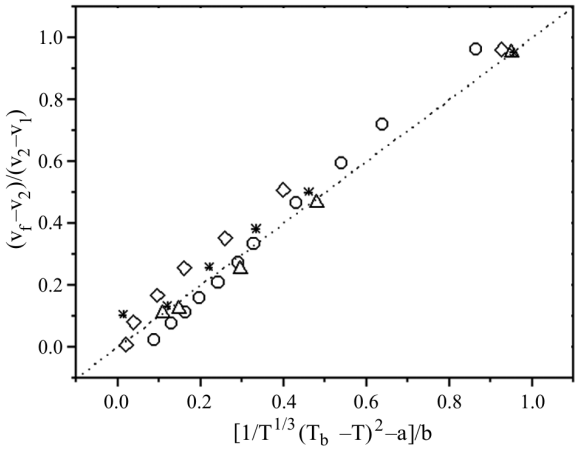

Fig. 4 Experimental results, for $T_2<T_0<T_1$; ○ – methanol, ◇ – ethanol, △ – propanol, * – butanol

The data are plotted, using dimensionless variables, in Fig. 4.

The scaling parameters a, b used in this plot correspond to

$$a = \frac{1}{T_2^{1/3}(T_b - T_2)^2} \tag{15}$$

$$b = \frac{1}{T_1^{1/3}(T_b - T_1)^2} - \frac{1}{T_2^{1/3}(T_b - T_2)^2} \tag{16}$$

and v_1, v_2 are the flame spreading velocities corresponding to the transition points $T_0=T_1$; $T_0=T_2$, respectively. The correlation coefficient of the linear regression shown in Fig. 4 is close to 0.96.

Thermocapillary assisted propagation regime: $T_3<T_0<T_2$

In this case, flame spreading is also uniform as in the regime described in the previous section, but the slope of the T_0–v_f diagram is now close to 1 cm s^{-1}. The formula

$$v_f \approx u_{nsg} \frac{\lambda_g \rho_g c_{pg}}{\lambda_l \rho_l c_{pl}} \left(\frac{\Delta T_g}{\Delta T_l}\right)^2 \tag{17}$$

predicts very low values of the flame spreading velocity in this region, compared to the experimentally observed ones. This circumstance can be explained by the enhancement of the flame spread rate by thermocapillary convection of heat that warms the liquid fuel ahead of the flame, thereby reducing the heat losses towards the condensed fuel. For $T_0>T_2$, thermocapillary convection is negligible and this assistance effect is absent, whereas for values of T_0 lower than T_2, thermocapillary convection becomes, progressively, more important for lower initial surface temperature, as Fig. 3 shows. This fact is reflected in the T_0–v_f diagram of Fig. 2 by a significant and abrupt variation in the slope (of one order of magnitude) when the transition temperature T_2 is crossed. This enhancing mechanism, that speeds up flame spreading, now becomes the driving mechanism. The situation in this regime is similar to the preceding one, but instead of considering the thermal conductive flux q_l in the liquid fuel, we should consider the convective heat flux in this phase when the thermocapillary vortex is present.

A purely thermal (non reactive) model, based on the thermocapillary effect has been proposed for flame spreading over liquid fuels [12]; according to this work the heat flux in the liquid phase, through the thermocapillary vortex, can be estimated as

$$q_l \approx \mathrm{Pr}^{1/2} S^{1/2} \mathrm{Re}\, \lambda_l \frac{\Delta T_l}{h} \tag{18}$$

([12], p. 48). Here Pr is the liquid Prandtl number, and

$$\mathrm{Re} = \frac{v_f h}{\nu_l} \tag{19}$$

is the characteristic channel flow Reynolds number, where h is the liquid fuel depth. Also, the dimensionless parameter S accounts for the thermocapillary effect and is defined as

$$S = \frac{|\sigma'|\Delta T_l}{\rho_l \nu_l v_f} \tag{20}$$

where $\sigma' = \mathrm{d}\sigma / \mathrm{d}T$ is the derivative of the fuel surface tension σ with temperature. The equation that gives us the heat flux q_l is in this case the result of an asymptotic analysis valid in the limit of large values of S [12]. When this convective heat flux is equated to the conductive heat flux entering from the gas phase q_g (identical to the result obtained in the previous regime) the following temperature dependence of the spreading velocity is obtained

$$v_f \approx \frac{1}{(T_b - T_0)^3} \tag{21}$$

In order to verify the adequacy of this relation a linear fit between the flame spreading velocity and the variable $1/(T_b–T_0)^3$ has been performed in this region with the data from the four alcohols in the 40 cm long channel, with Pyrex lateral walls. The experimental data have been plotted in Fig. 5, using dimensionless variables. The scaling parameters a', b' used in this plot correspond to

$$a' = \frac{1}{(T_b - T_3)^3} \tag{22}$$

$$b' = \frac{1}{(T_b - T_2)^3} - \frac{1}{(T_b - T_3)^3} \tag{23}$$

the correlation coefficient is close to 0.95.

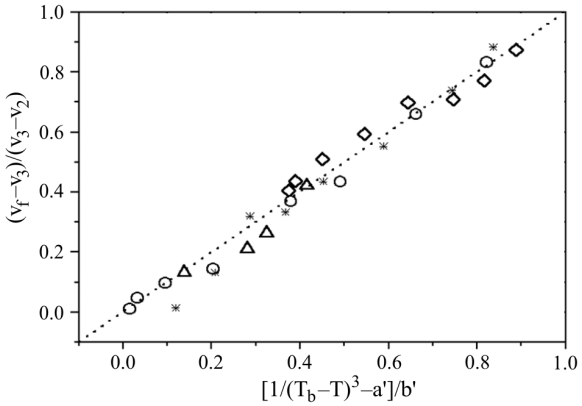

Fig. 5 Experimental results, for $T_3<T_0<T_2$; ○ – methanol, ◇ – ethanol, △ – propanol, * – butanol

Table 2 Experimental values of S for $T_0=T_2$

Channel	Methanol	Ethanol	Propanol	Butanol
Aluminium	33.1	38.9	27.9	54.7
Pyrex	34.6	46.1	24.0	28.8

As pointed out in [4], for sufficiently large values of S a recirculation bubble appears that enhances flame spreading. The values of S, for $T_0=T_2$ evaluated from experimental data are shown in Table 2. They have been obtained for all the alcohols used in the different experimental configurations. The length of the tray was 40 cm, and the material of the lateral walls as indicated. They result to be a decreasing function of the temperature T_0, and vary between 24.0 and 54.7, a result that validates the usage of equation that estimates q_l, which was derived for $S\approx O(10)>>O(1)$.

Finally, for fuel temperature values $T_0<T_3$, the steady but dynamic energy balance just described in the liquid fuel below the flame tip becomes unstable and flame spreading pulsation occurs.

Conclusions

The two different steady state spreading regimes, above and below the transition value $T_0=T_2$, have been experimentally characterized. For $T_0>T_2$, the flame spreading velocity has been shown to be controlled by the heat flow balance at the liquid fuel surface; flame spreading is described by the De Ris solid fuel-like model, as no detectable motions in the liquid fuel occur. For $T_3<T_0<T_2$, a preheating region has been observed in the fuel, whose size increases with decreasing temperatures (typically from an order smaller than 1 mm to another one bigger than 1 cm). In this region, flame spreading velocity follows the law predicted by the purely thermo-hydrodynamic non-reactive model proposed in [12].

The transition observed at temperature T_2, which corresponds to a transcritical bifurcation between two steady states, has shown to present common characteristics for all alcohols: weak dependence on the different experimental conditions tested in this work is observed.

When the fuel temperature is decreased below T_2, the assistance mechanism is reinforced as we decrease the initial fuel surface temperature, until the value $T_0=T_3$ is reached; at this point, the steady surface heat balance becomes unstable, and a pulsating behavior develops.

A theoretical approach of the physical mechanism driving the flame spreading in the pulsating regime, and its relation with the thermocapillary effect, for values $T_0\approx T_3$ is a possible subject for future work.

Also, the initial flame surface temperature T_0 results to be a control parameter of flame spreading velocity v_f that could be of interest in future research to improve fire safety conditions in fuel containers.

Acknowledgments

This work has been sponsored by the Spanish DGICYT (project number PB94-0385).

References

1 W. A. Sirignano and I. Glassman, Combust. Sci. Technol., 1 (1970) 307.
2 K. Akita, XIV. Symposium (International) on Combustion, The Combustion Institute, Pittsburgh 1973, pp. 1075–1083.
3 A. Ito, D. Masuda and K. Saito, Combust. Flame, 83 (1991) 375.
4 F. J. Miller and H. D. Ross, 'Liquid-phase velocity and temperature fields during uniform flame spread over 1-propanol", 8th International Symposium on Transport Processes, San Francisco, CA 1995.
5 F. A. Williams, Combustion Theory, 2nd Ed., Benjamin/Cummings Publishers, Menlo Park, CA 1985.
6 M. Furuta, J. Humphrey and A. C. Fernández-Pello, Phys. Chem. Hydrodynamics, 6 (1985) 347.
7 R. Schiller, H. D. Ross and W. A. Sirignano, Combust. Sci. Technol., 118 (1996) 203.
8 I. Glassman and F. L. Dryer, Fire Safety J., 3 (1980) 123.
9 C. Di Blasi, S. Crescitelli and G. Russo, XXIII. Symposium (International) on Combustion, The Combustion Institute, Pittsburgh 1990, pp. 1669–1675.
10 H. D. Ross and R. G. Sotos, XXIII. Symposium (International) on Combustion, The Combustion Institute, Pittsburgh 1990, pp. 1649–1655.
11 J. M. Miller and H. D. Ross, XXIV. Symposium (International) on Combustion, The Combustion Institute, Pittsburgh 1992, pp. 1703–1711.
12 F. J. Higuera and P. L. García Ybarra, Combust. Theory Modeling, 2 (1998) 43.
13 J. N. De Ris, XII. Symposium (International) on Combustion, The Combustion Institute, Pittsburgh 1969, pp. 241–252.
14 E. Degroote and P. L. García Ybarra, Eur. Phys. J. B, 13 (2000) 381.